

## Coupled numerical model of metal melting in an induction furnace: sensitivity analysis and validation of model

**Abstract.** In this paper, an accurate numerical model of coupled phenomena in an induction furnace applied in the modern metallurgy industry was formulated. In addition, an examination of material properties' influence on the melting process and the free surface shape in an induction furnace with a ceramic crucible was performed. The results showed insignificant influence of the most important properties on the free surface shape of the molten metal.

**Streszczenie.** Celem pracy było stworzenie dokładnego modelu numerycznego sprzężonego zjawiska topienia metalu w piecu indukcyjnym oraz identyfikacja wpływu własności materiałowych ciekłego metalu na uzyskiwane wyniki. Z tego powodu przeprowadzono szereg analiz wrażliwości przepływowych oraz elektromagnetycznych własności stopionego metalu. Zaobserwowano niewielki wpływ własności materiałowych na kształt powierzchni swobodnej, co świadczy o zasadności zastosowania uproszczeń w modelach numerycznych procesów topienia metalu w piecach indukcyjnych. **Dokładny model numerycznego sprzężonego zjawiska topienia metalu w piecu indukcyjnym**

**Keywords:** validation, coupled model, induction furnace, computational fluid dynamics

**Słowa kluczowe:** walidacja, model sprzężony, piec indukcyjny, numeryczna mechanika płynów

### Introduction

Modern metallurgy has to face numerous challenges such as providing materials of high purity and the thermal treatment of metals with a high melting temperature, e.g., titanium. Those challenges can be handled by employing induction furnace technology. To control, analyse and optimise the processes occurring in an induction furnace, both measurement and computational fluid dynamic (CFD) simulation techniques can be applied.

Some experimental and simulation results addressed in this work are available in the recent literature. A review demonstrates clearly that experimental studies are more advanced than the developed numerical approaches. Mathematical models have to deal with coupling of thermofluid and electromagnetic fields [1-5]. Usually, the angular direction is neglected; either the axisymmetry [6] or a small 3-D segment with appropriately defined periodicity conditions [7] is examined. In general, the melted metal in a crucible is mixed because of the effect of electromagnetic forces. As a result, a turbulent flow is evoked. This means that any mathematical model has to solve the turbulence problem. The most commonly used formulations are those based on the Reynolds-averaged Navier-Stokes (RANS) model. One paper [8] gives an analysis of the influence of different turbulence equations on the shape of the free surface of liquid metal. Turbulence intensity and its impact on the evaporation of components of the melt were examined as well [9]. In both of these papers, only averaged turbulence equations are solved; however, the current trend is to use more sophisticated techniques, able to reproduce the behaviour of the fluid in the near-surface domains. Large eddy simulations (LES) [10] and the Reynolds Stress Model are good examples of such approaches. Beyond geometrical representation and flow equations, thermal properties are crucial in simulations. Unfortunately, even small additions to alloys can change them drastically. Therefore, it is necessary to examine the influence of a particular property on the final numerical solution.

The main purpose of this paper is to investigate numerically the shape of liquid metal free surface as a result of a material property sensitivity analysis. The viscosity, surface tension, contact angle and resistivity of molten aluminium were examined in the coupled simulation of electromagnetic and flow fields. The final results were compared with measurement data showing insignificant

influence of material properties on the numerical results. The most impactful factor was the resistivity of aluminium.

### Measurements

Because of the high temperature of liquid metal inside the crucible, it is quite challenging to perform experiments. For this reason, contactless methods have to be used. In the course of the measurement campaign for a given current of the inductor, its position and filling fraction of the crucible, the following parameters can be monitored.

1. The shape of the free surface and its linear profile using a 3-D camera and laser technique.
2. The velocity on the liquid metal surface, assessed by tracking the local singularities and markers using a high-resolution, high-speed camera. This measurement yields quantities directly associated with the mass transfer on the metal-gaseous phase interface.
3. Temperature field on the surface assessed by an IR camera or by a two-colour pyrometer.

Besides these measurements, it is possible to determine the chemical composition of the melt. Taking samples can be accomplished during the purification process. Thus, the investigation carried out can yield necessary data for the validation of the part of the coupled model that concerns the transient transport of impurities of additives from the bath to its surrounding.

The capabilities of the measurement site allow us to measure the shape of molten metal under different operating conditions. For that reason the laser technique was applied. The reflection of the laser beam from metal surface was registered. Using triangulation method, we determined the metal distance from the detector. This scheme was repeated for several points of the metal surface. As a result, information about the shape of the free surface was acquired. The measurement site included a coil around the ceramic crucible in which the sample of metal was placed (Fig. 1). The height of the crucible was 200 mm. It had a conical shape with a larger radius of 62 mm and a smaller radius of 30 mm. Experiments on this rig were conducted for three positions of coil and a few values of the current. In this study, only one position and current were examined. The bottom part of the coil was located 51.5 mm above the bottom of the crucible. A current of 1000 A was set. All settings were defined in the coupled numerical model.



Fig. 1. Measurement site with ceramic crucible and liquid aluminium

### Mathematical model

To simplify the examined crucible, only axial and radial forces were assumed to act on the liquid metal. Therefore, the geometry was defined as 2-D axisymmetrical. The thermofluid domain (Fig. 2) was restricted to the walls of the crucible and it contained the air and liquid metal phases. The electromagnetic (EMAG) model included a crucible with liquid metal, coil and surrounding air. It was necessary to obtain the electromagnetic force distribution in the liquid metal.

For that reason, different discretisations were used for both methods. The finite volume method requires a fine quadrilateral grid, but for the finite element method coarser mesh is enough. The CFD submodel was divided into 24 000 quadrilateral elements, and the EMAG domain was split into 12 000 triangles. Both grids were examined in terms of numerical stability and results independence.

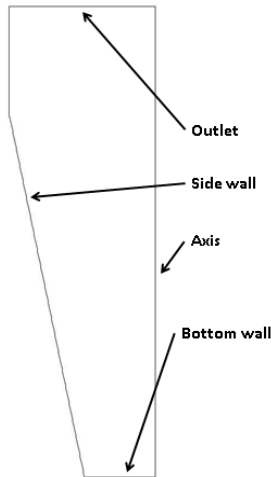


Fig. 2 Computational domain and boundary condition types in the CFD submodel

The process of metal melting in a crucible is highly unsteady. Therefore, all the computations were carried out in a transient mode. To describe fully the analysed electromagnetic problem, the magnetic vector potential equation was applied:

$$(1) \quad \nabla \times \left( \frac{1}{\mu} \nabla \times \mathbf{A} \right) + j\omega\sigma\mathbf{A} = \mathbf{J}_s$$

where  $\mu$  is the magnetic permeability,  $\sigma$  is the electric conductivity,  $\omega$  is the angular frequency and  $\mathbf{J}_s$  is the current density source.

On the basis of the distribution of the magnetic vector potential  $\mathbf{A}$ , a distribution of the magnetic induction  $\mathbf{B}$  (Eq. 2), the eddy current densities  $\mathbf{J}$  (Eq. 3) and the density of electromagnetic force that acts on a liquid metal  $\mathbf{f}_e$  (Eq. 4) can be determined:

$$(2) \quad \mathbf{B} = \nabla \times \mathbf{A}$$

$$(3) \quad \mathbf{J} = -j\omega\sigma\mathbf{A}$$

$$(4) \quad \mathbf{f}_e = \frac{1}{2} \text{Re}(\mathbf{J} \times \mathbf{B})$$

The fluid dynamics model was described by Navier-Stokes equations. For transient 2-D axisymmetrical problems, these equations are as follows:

$$(5) \quad \begin{aligned} & \frac{\partial}{\partial t}(\rho v_x) + \frac{1}{r} \frac{\partial}{\partial x}(r \rho v_x v_x) + \frac{1}{r} \frac{\partial}{\partial r}(r \rho v_r v_x) = -\frac{\partial p}{\partial x} \\ & + \frac{1}{r} \frac{\partial}{\partial x} \left[ r \mu \left( 2 \frac{\partial v_x}{\partial x} - \frac{2}{3} (\nabla \cdot \mathbf{v}) \right) \right] + \frac{1}{r} \frac{\partial}{\partial r} \left[ r \mu \left( \frac{\partial v_x}{\partial r} + \frac{\partial v_r}{\partial x} \right) \right] \\ & + \rho g + F_x \end{aligned}$$

$$(6) \quad \begin{aligned} & \frac{\partial}{\partial t}(\rho v_r) + \frac{1}{r} \frac{\partial}{\partial x}(r \rho v_x v_r) + \frac{1}{r} \frac{\partial}{\partial r}(r \rho v_r v_r) = -\frac{\partial p}{\partial r} \\ & + \frac{1}{r} \frac{\partial}{\partial x} \left[ r \mu \left( \frac{\partial v_r}{\partial x} + \frac{\partial v_x}{\partial r} \right) \right] + \frac{1}{r} \frac{\partial}{\partial r} \left[ r \mu \left( 2 \frac{\partial v_r}{\partial r} - \frac{2}{3} (\nabla \cdot \mathbf{v}) \right) \right] \\ & - 2\mu \frac{v_r}{r^2} + \frac{2}{3} \frac{\mu}{r} (\nabla \cdot \mathbf{v}) + F_r \end{aligned}$$

where  $\rho$  is the density,  $t$  is the time,  $x$  and  $r$  are the axial and radial coordinates, respectively,  $v$  is the velocity vector,  $g$  is the gravitational acceleration vector,  $\mu$  is the dynamic viscosity and  $F$  is the Lorentz force vector.

To track the position of the metal surface, it was necessary to implement the multiphase model. In this work, the volume of fluid (VOF) model with an explicit approach was performed. In this methodology, the conservation equation is solved for the volume fraction:

$$(7) \quad \frac{\alpha_q^{n+1} \rho_q^{n+1} - \alpha_q^n \rho_q^n}{\Delta t} V + \sum_f (\rho_q U_f^n \alpha_{q,f}^n) = 0$$

where  $\alpha_q$  is the volume fraction of the current ( $n+1$ ) and the previous ( $n$ ) time step and  $U$  is the volume flux.

The closures of numerical domains were boundary conditions. For both models, the axis symmetry appeared. In electromagnetic simulations zero potential value was assumed on the domain boundaries. For the crucible in the CFD model, walls without slipping were prescribed. The velocity profile near the wall was solved by using standard wall functions of RANS models. The top of the model was described as the pressure outlet.

To converge fully the numerical computations, two seconds of the process were simulated. This time can be divided into stages. The initial condition was the flat surface of the melted metal. Then, because of the surface tension the natural meniscus occurred. In the third step, the Lorentz force field compressed the liquid and resulted in a slimmer shape of the free surface. Then, after some vertical motions of the free surface, the final stage of the meniscus appeared.

According to the presented equations, the information about the electromagnetic force coordinates needs to be transferred to the thermofluid solver. In the opposite

direction, the shape of liquid metal is delivered. On the basis of the previous sensitivity analysis, the amount of transfers was optimised and its frequency was set to one per 100 time steps. Because of rapid changes in the free surface during computations a small value of the time step was needed. After examination of several cases, the time step of 0.0001 s was used. The coupling of electromagnetic and thermofluid fields was realised in Ansys Fluent software with the user defined functions (UDF) capability. This own code was responsible for controlling and exchanging information between the two solvers: electromagnetic (Ansys Mechanical APDL) and fluid dynamics (Ansys Fluent).

To simplify the coupled model, the influence of the temperature distribution on the material properties was neglected. It was assumed that once the metal is melted, its temperature is uniform. However, the value of the property can affect the flow field and the shape of the free surface. Therefore, the influence of the liquid aluminium viscosity, surface tension, contact angle and the electric resistivity was studied. The base values of the molten material of these properties are as follows: the dynamic viscosity  $\mu = 0.0015$  Pa·s, the surface tension coefficient  $\gamma = 0.9$  N/m, the contact angle  $\theta = 120^\circ$  and the electric resistivity  $\rho = 2.77 \cdot 10^{-7}$   $\Omega \cdot m$ . These values are averaged for liquid aluminium at a temperature 1000 K. To analyse the impact of a particular property, each value was increased and decreased by 10%. Then all three cases were compared with the measurement data.

## Results

The electric resistivity of aluminium was the first examined property. The results of numerical simulations and measurements are compared in figure 3. The differences between computations and experiments in the area near the crucible wall were caused by chemical reactions. The oxidation of aluminium was intense because of the high temperature and lack of inert gases. The mathematical model does not consider the oxidation process, and therefore the impurities are not presented in the simulation results. The oxides fell down next to the wall, resulting in the metal flat surface in this area. In the middle part of the meniscus, the simulation results are fully consistent/aligned with the measurement data. The top fragment of the metal surface was completely inaccurate. The inaccuracy of the numerical results obtained in this context may derive from the experimental methodology which did not provide an averaging scheme.

The impact of the electric resistivity on the shape of the metal surface was observed especially in the top of the meniscus. The decrease of aluminium resistivity produced the higher and slimmer free surface shape. However, the difference between consecutive values of the electric resistivity was not significant.

In order to identify the effect of the contact angle and surface tension coefficient on the molten metal shape, further simulations were performed. The results are presented in figure 4 and figure 5, respectively. The impact of the contact angle is only visible near the crucible wall. The smaller its value, the higher the contact point position of the melted aluminium and crucible wall. Nonetheless, the influence is minimal. The corresponding situation was observed for the sensitivity study of the surface tension coefficient. Differences in the simulated shape were observed on the peak of the metal meniscus and in its middle area. This slight impact of both properties allows one to use coarse data describing the metal and alloys without incurring large errors in the final solution. It also means that the source term in Navier-Stokes equations is the most crucial factor regarding the shape of the molten metal.

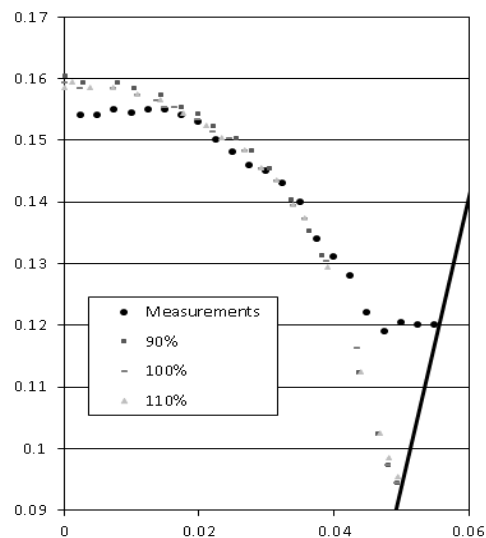


Fig. 3 Effect of the liquid aluminium electric resistivity on the metal free surface

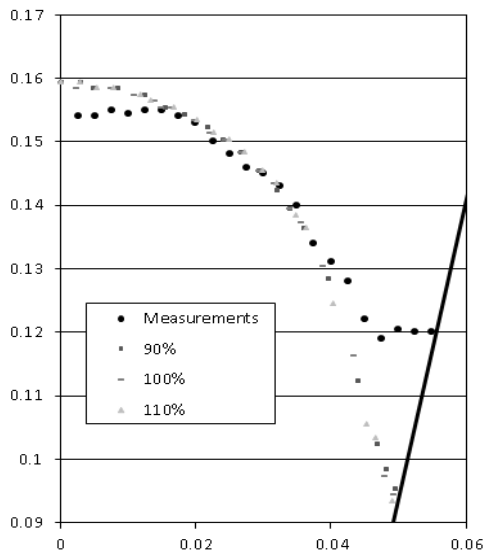


Fig. 4 Effect of the liquid aluminium and wall contact angle on the metal free surface

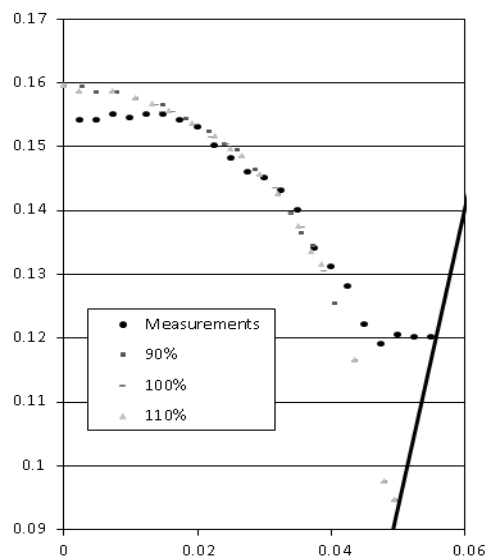


Fig. 5 Effect of the liquid aluminium surface tension coefficient on the metal free surface

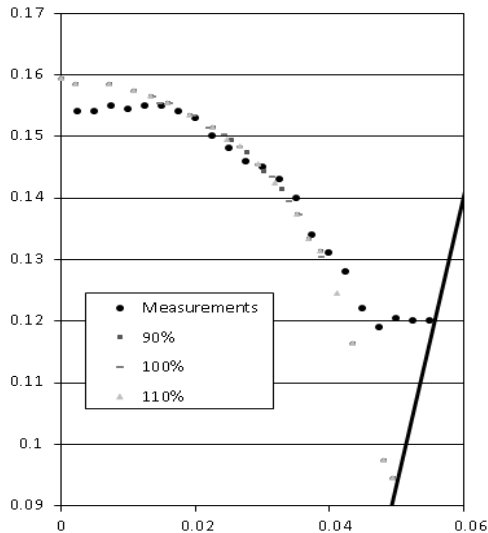


Fig. 6 Effect of the liquid aluminium viscosity on the metal free surface

The dynamic viscosity is strongly dependent on temperature. This led to imprecise values in the simplified isothermal mathematical model. To examine the influence of these inaccuracies on the described model, a sensitivity analysis was conducted. The results of numerical computations obtained for different viscosity values and compared with the experiments are presented in figure 6. The featured cases almost do not differ from each other. There is almost no effect of viscosity on the shape of the molten metal.

### Conclusions

This paper describes a coupled numerical model of the metal melting process in an induction furnace. Sensitivity analysis of material properties' effect on the shape of liquid aluminium was carried out. The electric resistivity of molten metal has the largest impact on the shape of the free surface. However, it was shown that the shape change is still insignificant. The other tested properties indicated even smaller impact. The Lorentz force which is the source term in the momentum conservation equation played the most crucial role in the meniscus forming on the molten metal.

In this work, the simulations were also validated against the experimental data. This comparison clearly showed that the model can only practically predict the actual shape of the molten aluminium. The further improvement of the numerical description is needed for implementation of the third coordinate, energy equations, to examine the whole process of metal melting in crucibles, etc. In addition, more experimental tests need to be carried out.

This work was partially supported by the statutory research fund of the Faculty of Power and Environmental Engineering, SUT, Poland.

**Authors:** mgr inż. Piotr Buliński, Politechnika Śląska, Instytut Techniki Ciepłej, ul. Konarskiego 22, 44-100 Gliwice, E-mail: [piotr.bulinski@polsl.pl](mailto:piotr.bulinski@polsl.pl); dr hab. inż. Jacek Smółka, Politechnika Śląska, Instytut Techniki Ciepłej, ul. Konarskiego 22, 44-100 Gliwice, E-mail: [jacek.smolka@polsl.pl](mailto:jacek.smolka@polsl.pl); dr inż. Sławomir Golak, Politechnika Śląska, Katedra Informatyki Przemysłowej, ul. Krasińskiego 8, 40-019 Katowice, E-mail: [slawomir.golak@polsl.pl](mailto:slawomir.golak@polsl.pl); dr hab. inż. Roman Przyłucki, Politechnika Śląska, Katedra Informatyki Przemysłowej, ul. Krasińskiego 8, 40-019 Katowice, E-mail: [roman.przylucki@polsl.pl](mailto:roman.przylucki@polsl.pl).

### REFERENCES

- [1] Bojarevics V., Harding R.A., Wickins M., Experimental and numerical study of the cold crucible melting process, Proceedings of the Third International Conference on CFD in the Minerals and Process Industries (2003), CSIRO.
- [2] Songa J.H., Mina B.T., An electromagnetic and thermal analysis of a cold crucible melting, International Communications in Heat and Mass Transfer, 32 (2005), pp. 1325-1336.
- [3] Spitans S., Jakovics A., Baake E., Nacke B., Numerical modelling of free surface dynamics of conductive melt in the induction crucible furnace, Magnetohydrodynamics, 46 (2010), pp. 317-328.
- [4] Spitans S., Jakovics A., Baake E., Nacke B., Numerical modelling of free surface dynamics of melt in an alternate electromagnetic field, Magnetohydrodynamics, 4 (2011), pp. 461-473.
- [5] Spitans S., Jakovics A., Baake E., Nacke B., Numerical modelling of free surface dynamics of melt in alternate electromagnetic field, Journal of Iron and Steel Research International, 19 (2012), pp. 531-535.
- [6] Yang J., Chen R., Ding H., Guo J., Han J., Fu H., Thermal characteristics of induction heating in cold crucible used for directional solidification, Applied Thermal Engineering, 59 (2013), pp. 69-76.
- [7] Quintana I., Azpilgain Z., Pardo D., Hurtado I., Numerical Modeling of Cold Crucible Induction Melting, Proceedings of The COMSOL Conference (211), Boston, USA.
- [8] Buliński P., Smółka J., Golak S., Przyłucki R., Blacha L., Białecki R., Palacz M., Siwiec G., Effect of turbulence modeling in numerical analysis of melting process in an induction furnace, Archives of Metallurgy and Materials, 60 (2015), pp. 1575-1579.
- [9] Adler K., Schwarze R., Galindo V., Numerical modelling of the evaporation process of an electromagnetically stirred copper melt, Proceedings of the FLUENT CFD Forum (2005), Bad Nauheim, Germany.
- [10] Umbrasko A., Baake E., Nacke B., Jakovics A., Numerical studies of the melting process in the induction furnace with cold crucible, COMPEL: The International Journal for Computation and Mathematics in Electrical and Electronic Engineering, 27 (2008), pp. 359-368.